Available online at www.sciencedirect.com
ScienceDirect
Thermochimica Acta 467 (2008) 63–72
thermochimica acta
www.elsevier.com/locate/tca

Encapsulation of phase change materials by complex coacervation to improve thermal performances of woven fabrics

Emel Onder [a,1], Nihal Sarier [b,*], Erhan Cimen [a]

[a] *Istanbul Technical University, Department of Textile Engineering, Gumussuyu, Istanbul 34437, Turkey*
[b] *Istanbul Kultur University, Department of Civil Engineering, Bakirkoy, Istanbul 34156, Turkey*

Received 16 August 2007; received in revised form 1 November 2007; accepted 6 November 2007
Available online 21 November 2007

Abstract

In this study, three types of paraffin waxes suitable for textile applications, namely *n*-hexadecane, *n*-octadecane and *n*-nonadecane were encapsulated through complex coacervation of natural and biodegradable polymers, gum arabic–gelatin mixture, in order to investigate their heat storing or releasing capacities, their durability as well as their practicable thermal performances when integrated into woven fabrics by coating.

FT-IR results of capsules have presented the proofs of successful complex coacervation of PCMs. Most of the coacervates withstood considerable centrifugal forces in the leakage test and compression in coating applications of fabrics without resulting in any oil leak. DSC curves taken at 10 °C min^{-1} and calorimeter measurements at the heating rate of 0.5–1 °C min^{-1} of coacervates illustrate substantial endothermic enthalpies in the intervals corresponding to the phase transition interval of the paraffin wax used in a particular core, and tend to increase whereas the dispersed PCM contents in emulsions are relatively higher. One of the coacervates of *n*-hexadecane performed the enthalpy value of 144.7 J g^{-1}, while another coacervate containing *n*-octadecane provided 165.8 J g^{-1} and the coacervate including *n*-nonadecane presented 57.5 J g^{-1} enthalpy. When coacervates were incorporated with woven fabrics, their feasible thermal performances appeared to be related to both actual paraffin wax content of the coacervate and the incorporation amount of it by the coating application. The energy absorption capacities of the coacervate added fabrics were found to be 2.5–4.5 times enhanced relative to the reference fabric for particular temperature intervals.

Keywords: Complex coacervation; Gelatin; Gum arabic; Paraffin waxes; Encapsulation; DSC; FT-IR

1. Introduction

The field of textile has always been one of the main application domains of scientific researches, newly received great attention to design and develop functional and smart materials. Textiles has replaced many other conventional materials in our daily life and in several technical fields thanks to the diversity reached and added functions achieved in recent years. Thus, the use of textile materials has been widening rapidly to assist the survivability and to improve the quality in all living areas of human being and of technology. Among the emerging technologies, encapsulation of phase change materials (PCMs) has been grown up to provide significantly enhanced thermal management for coolants, textile fibers and surfaces, foams, composites and coatings in application to avionics, spacesuits, buildings, machine coolants, electronics, apparel, packaging, food, agriculture, etc. [1–11].

A large number of possible candidates for latent heat storage in a broad temperature range have been reported in literature [12–15]. Linear chain hydrocarbons known as paraffin waxes, composed of *n*-alkanes, CH_3–$(CH_2)_n$–CH_3, are widely utilized as PCMs. Some of these waxes offering large thermal storage densities have melting temperatures lying in practical ranges suitable for thermal comfort maintenance of textiles [7,16–20]. Conversely, the crystallization of C_nH_{2n+2} chain releases a large amount of latent heat while cooling. Both the melting point and the heat of fusion increase with increasing chain length. Paraffin waxes are chemically stable, showing no phase segregation with minimum sub-cooling during repetitive phase transitions, nontoxic, noncorrosive, odorless and easily available.

The encapsulation of PCM is the most advantageous technique to merge the expected enriched heat performance with

* Corresponding author. Tel.: +90 2124984488; fax: +90 2126618563.
E-mail addresses: onderem@itu.edu.tr (E. Onder), n.sarier@iku.edu.tr (N. Sarier).
[1] Tel.: +90 2122931300x2496.

0040-6031/$ – see front matter © 2007 Elsevier B.V. All rights reserved.
doi:10.1016/j.tca.2007.11.007

Table 1
Materials used in complex coacervation of PCMs

Material	Its function in coacervation
Polysaccharide (gum arabic, acacia)	Shell material
Protein (gelatin)	Shell material
Dodecyl sulfate sodium salt (SDS) ($C_{12}H_{25}OSO_2ONa$)	Emulsifier, surfactant
Potassium peroxodisulfate ($K_2O_8S_2$)	Electrolyte
Sodium thiosulfate ($Na_2S_2O_3$)	Electrolyte
n-Hexadecane ($CH_3(CH_2)_{14}CH_3$)	Core material, PCM
n-Octadecane ($CH_3(CH_2)_{16}CH_3$)	Core material, PCM
n-Nonadecane ($CH_3(CH_2)_{17}CH_3$)	Core material, PCM
Formaldehyde (H_2CO) (30.0 mol^{-1})	Binder, cross linker
Sodium carbonate (Na_2CO_3)	Electrolyte for capsule precipitation

the other textile qualifications on the same product. The incorporation of PCMs into textiles in the form of a shell-core matrix brings many opportunities such as prevention of PCM dispersion in the structure, less evaporation and minimum interaction with the environment, increased heat transfer area, long shelf-life on a garment for normal fabric-care processes, no adverse effect on the textile properties so on [7,16,19,21]. The encapsulated PCM is usually embedded in a conductive medium. The characteristics of capsules, phase change material and conductive medium can be designed so as to provide the enhanced thermal management in a wide variety of applications.

The controllable encapsulation processes are mostly based on simple or complex coacervation as well as interfacial or in situ polymerization techniques [21–26]. Coacervation is mainly the separation into two liquid phases as in water-in-oil or oil-in-water colloidal systems [IUPAC 1997] [27] where the latter is appropriate for PCM encapsulation. The complex coacervation can be accomplished by the interaction of two oppositely charged colloids, in which the core material in dispersed form is added to the polymer solution, and the mixture is then suspended in an aqueous phase containing a surface-active agent. The complex coacervation techniques dealing with the gelatin–gum arabic system have been studied extensively in areas including carbonless copying paper, and drug, nutritional supplementary, flavoring and fragrance encapsulation, etc. Encapsulation of paraffin-waxes by complex coacervation is a recent topic of study as energy storage material [28–35].

The first aim of this study is to fabricate encapsulated PCMs through complex coacervation of natural and biodegradable polymers, gum arabic–gelatin mixture, in order to investigate their heat storing or releasing capacities as well as their durability. The associated aim is to examine the practicable thermal performances of these coacervates when incorporated with woven fabrics.

2. Experimental

2.1. Encapsulation of PCMs

This part of the experimental work copes with the complex coacervation of a protein and a polysaccharide, encapsulating a phase change material, and the characterization of chemical composition, durability and thermal behavior of the composites manufactured. Materials used in complex coacervation, are all by Merck are given in Table 1.

Two natural polymers were used as oppositely charged colloids to form the shell encircling the core. Gum arabic (GA) is a complex polysaccharide extruded from the African tree acacia senegal. It is a complex and variable mixture of polysaccharides and glycoproteins where heavily branched galactose/arabinose side chains linked to a main polypeptide of galactan chain is shown in Fig. 1. GA is negatively charged above pH of 2.2 ultimately providing good emulsifying properties. Gelatin is a heterogeneous mixture of single or multi-stranded polypeptides, namely glycine, proline and 4-hydroxyproline residues, each containing between 300 and 4000 amino acids (see Fig. 2). Type A gelatin that we used in the study is a product of acid pretreatment and has the isoelectric point at around pH of 8. The amphoteric nature of the molecules endows them with useful emulsification and coacervate formation. On dehydration, irreversible conformational changes take place in the stable capsule-shell formation.

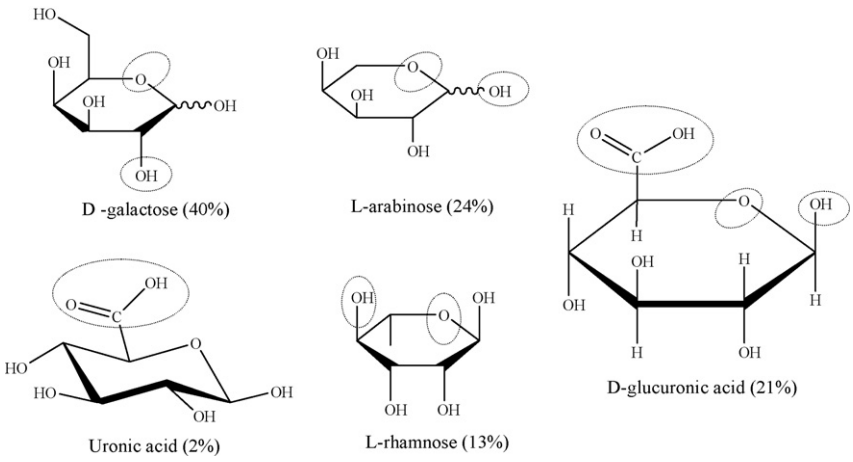

Fig. 1. Chemical structures and percentages D-galactose, L-arabinose, D-glucuronic acid, L-rhamnose and uronic acid forming the mixture of gum arabic (some of the functional groups responsible for polymerization during complex coacervation are encircled).

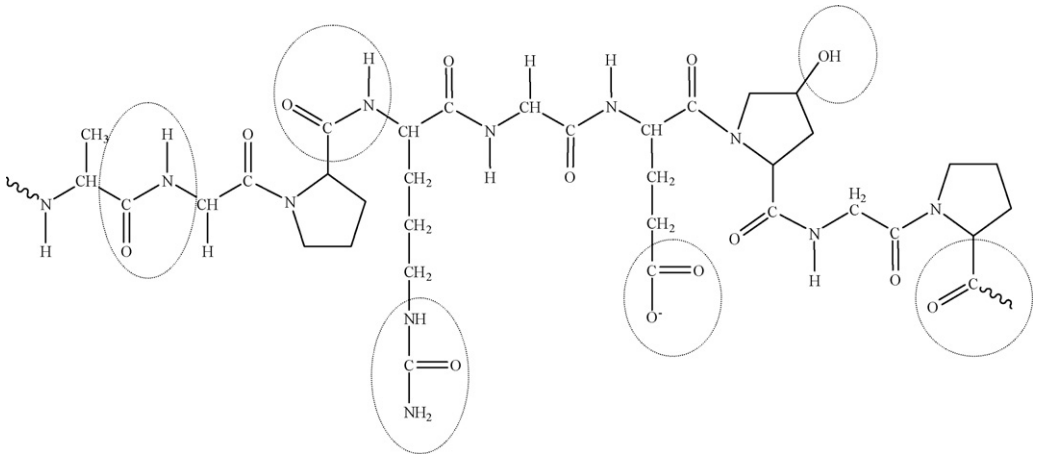

Fig. 2. Chemical structure of gelatin (some of the functional groups responsible for polymerization during complex coacervation is encircled).

Three types of paraffin waxes suitable for textile applications, namely *n*-hexadecane, *n*-octadecane and *n*-nonadecane were decided to be capsulated material. The phase change enthalpies of *n*-hexadecane and *n*-octadecane were obtained in DSC analyses as 185 J g^{-1} in between 10 °C and −26 °C (peak at 22 °C) and 234 J g^{-1} in between 26 °C and −44 °C (peak at 35.6 °C), respectively [7,36]. Furthermore, *n*-nonadecane showed rotator phase transition from a fully ordered crystal to a crystal that retains translational order but exhibits dynamic orientational disorder (22.8–27.4 °C; 47.9 J g^{-1}) and solid–liquid phase transition (27.4–36.6 °C; 146.4 J g^{-1}) corresponding to the total heat of 194.3 J g^{-1} as obtained from DSC when heated from −50 °C to 40 °C at 10 °C min^{-1} (see Fig. 7) [IUPAC 1994] [37].

Production parameters of insoluble protein–polysaccharide copolymer shell encircling PCM droplets were chosen as pH of colloid system, protein–polysaccharide-surfactant molar ratio, temperature of the system during and after coacervate formation, stirring rates of the mixtures and concentrations of electrolyte solutions. Then the complex coacervation was conducted by the following procedure: one unit gelatin was dissolved in ten units of distilled water above 45 °C and stirred at 1000 rpm for 10 min. At this stage, saturated solution of SDS, 0.5% $K_2S_2O_8$ (aq.), 0.5% $Na_2S_2O_3$ (aq.) in the volume ratio of 12:1:1 were added drop by drop. One unit GA was successively mixed into the emulsion for the next 15 min under the same conditions. The pH of homogenized colloidal dispersion was adjusted to 4–5. Afterwards, the core material, in varying ratios for a series of experiments as shown in Table 2, was put into the mixture and the stirring rate was increased to 1600 rpm for the subsequent 1 h while still keeping the temperature at a level above the solving temperatures of colloids and melting temperature of PCM. In turn, a few drops of 10% sodium carbonate solution were added to dissociate the polyelectrolyte complexes at 500 rpm for 5 min. Then, 10% Na_2CO_3(aq.) by half of reaction mixture was poured into the coacervate in the ice bath at about 5 °C. To complete the phase separation, pH was adjusted to 9–10 and 5 mL of 37% formaldehyde was put for fixation. The coacervate was recovered after washing with water repeatedly, filtering and drying.To characterize the thermal behavior of the samples given in Table 2, DSC analyses were conducted on Perkin-Elmer Diamond DSC under normal atmospheric conditions. During DSC analyses, test specimens were first held at −50 °C for 2 min and then heated from −50 °C to 40 °C at 10 °C min^{-1}, which is common for polymer analysis [7,32,38]. Consecutively, the samples were held at 40 °C for 1 min and then cooled from 40 °C to −50 °C at 10 °C min^{-1}. In addition, a computer aided data acquisition system connected to a thermocouple and a double-wall calorimeter was used to measure thermal responses of 2–3 g coacervates against those of the same amount of distilled water when heating from 5 °C to 40 °C at a relatively lower rate of 0.5–1 °C min^{-1}. In order to identify the chemical structure of coacervates composed of shell and core materials, the infra red transmission spectra of specimens, dispersed in KBr pellets, were performed on Perkin-Elmer Fourier Transform Infrared (FT-IR) Spectrophotometer in between the wave numbers of 4000 cm^{-1} and 450 cm^{-1}.

The leakage behavior of coacervates was examined by the centrifugal shear force test [36]. Two grams of coacervate and 4 mL of water were put into a test tube. Tubes were centrifuged at 400 rpm for 4 h at room temperature and then stayed overnight in the refrigerator at 4 °C. Finally, the supernatant samples were controlled if there was any oil–water phase separation.

2.2. Coacervate incorporation into the woven fabrics

A coating method was applied to incorporate Coacervates II and III with a 100% cotton, 2/1 twill fabric, woven from

Table 2
Coacervates produced

Type of coacervate	Core PCM	The dispersed content in the emulsion (%)
Control	–	–
Coacervate I	*n*-Hexadecane	40
Coacervate II	*n*-Hexadecane	60
Coacervate III	*n*-Hexadecane	80
Coacervate IV	*n*-Octadecane	40
Coacervate V	*n*-Octadecane	60
Coacervate VI	*n*-Octadecane	80
Coacervate VII	*n*-Nonadecane	60

Table 3
Coating applications to the fabric samples

Type of coating	The contained coacervate type	Coating material to coacervate mixing ratio (mass to mass)	Incorporated coacervate % in the coated fabric sample
CF1	Coacervate II (60% *n*-hexadecane)	1:1	9.5
CF2	Coacervate II (60% *n*-hexadecane)	1:1	15.6
CF3	Coacervate II (60% *n*-hexadecane)	1:1.5	22.5
CF4	Coacervate III (80% *n*-hexadecane)	1:1	9.5

16/1 Ne warp and 12/1 Ne weft yarns at densities of 35 ends/cm × 18 picks/cm, weighing 276 g/m^2. Coating material was water soluble synthetic dispersion, commercially available for woven apparel fabrics, that was polyurethane based, anionic, of 9.5–10 pH value and with 45–48% active content. Fixing agent comprising melamine resins with low formaldehyde content was used for cross linking, which was miscible in water, nonionic and of 8–9 pH value.

Recipes were prepared for 1:1 and 1:1.5 mixtures of the coating material and the coacervate as shown in Table 3. Ten units coating material were stirred at 600 rpm for 5 min and then 10 or 15 units coacervate were mixed while increasing the stirring rate up to 1000 rpm for the next 5 min. After adding 5% foaming agent, the dispersion was processed at 1500 rpm stirring rate for another 15 min. 1.5% fixing agent was blended and stirring rate was halved for the last 2–3 min.

The preparation was applied to the fabric sample, cut into 30 cm × 30 cm piece, by a roller over blanket available on a laboratory type printing machine so that the pressure and the speed of roller were adjusted to be the lowest, not to give any damage to the capsulated material. Coated fabric samples were fixed in a drying oven for 15 min at a temperature increased gradually from 60 to 80 °C and then conditioned for the subsequent 24 h. To determine the actual incorporation percentages of the coacervates which also depend on the coating thickness transferred to the sample, coated and uncoated fabric pieces were weighed. The computer aided thermocouple and calorimeter system mentioned above was used here again to analyze the coated samples' thermal behavior against the uncoated ones.

3. Results and discussion

3.1. Characterization of coacervates by FT-IR spectra evaluations

Analyses results of FT-IR spectra of Coacervates II, III, V–VII and Control are summarized in Table 4, and typical three curves are presented in Fig. 3 in order to explain the characteristics of transmission bands and the relative intensities (ΔT %) of the samples. There is no distinctive transmission band at 3600–3000 cm^{-1} in all spectra, matching to free H_2O, since the residual water was removed by vacuum drying during experimental analyses. The spectrum of Control represents all the characteristic bands of polysaccharide–protein copolymer [39,40].

The ionized carboxyl groups of, $O = \underset{I}{C} - O^-$ demonstrated by stretching bands of high intensities at 2000–1700 cm^{-1} are the evidence of successful complex coacervation as a result of reaction between polysaccharide (GA) and protein (gelatin). Similarly, the peaks at 1655–1653 cm^{-1} are associated with the groups of –C–O–C (sugar)and –NH_2 (protein), and the peaks at 1561–1559 cm^{-1} are attributed with amine groups. Besides, their strength decreased to some extent since paraffin waxes in emulsions were likely to increase the micelle formation, and the role of SDS and other surfactants, here, took place in a way to build up an attraction to the oil phase with their organophilic ends and to the water phase with their hydrophilic ionic ends. Consequently, oppositely charged gelatin–GA copolymer chains achieved encapsulation of PCMs by encircling the oil droplets. There are similar falls in the transmission intensities of –C–O–C bonds in sugar rings at the wave numbers of 1507 and 1143 cm^{-1}as a result of micelle formation. Changes in transmission bands for the bending groups of –CH_3–CH_2–, at 1179 cm^{-1}, −1161 cm^{-1} and at 1057–1048 cm^{-1} for all coacervates, were due to the discontinuity of copolymer chains caused by PCM addition to the structure.

On the other hand, linear hydrocarbon chains in all coacervates showed a general tendency of bending due to the capsule formation emerged from the broad bands of –CH_2, –CH at 1459–1457 cm^{-1} in conjunction with the peak occurrences in various intensities. IR spectrum of Coacervate III follows a distinct course at high intensities within the broad range of 900–600 cm^{-1} differing from that of Control. The peaks occurred at 854–852 cm^{-1} and the sharp ones at 671–668 cm^{-1}, characterized by –CH2, –CH groups, stress the successful *n*-hexadecane trapping in gelatin–GA coacervate, actually not available in the IR spectrum of Control [15–17].

Visual differences observed in optical microscope images of Coacervate II and Control, given in Fig. 4a and b, can be

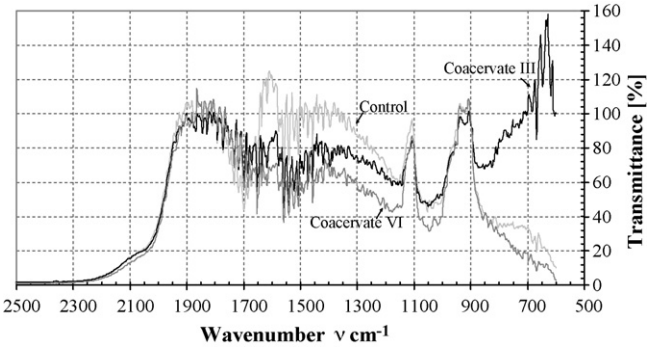

Fig. 3. FT-IR spectra of Coacervates III, VI and control between the wavenumbers of 2500 cm^{-1} and 500 cm^{-1}.

Table 4
Characteristics of transmission bands and the relative intensities (ΔT %) of FT-IR spectra

Vibrating group	Type of vibration	Wave number (ν cm^{-1})	Transmittance (ΔT %)					
			Control	II	III	V	VI	VII
–CH_2; –C–H	Stretching;	2942	1.7	1.8	1.6	0.7	0.7	1.2
–CH_2; –C–H	Stretching	2425	1.4	1.2	1.7	0.8	1.2	1.3
$O=\underset{I}{C}-O^-$	Ionized carboxyl group, stretching	1734	45.9	46.7	69.6	46.1	68.6	70.3
$O=\underset{I}{C}-O^-$	Stretching	1700–1699	43.7	35.6	64.8	38.3	60.3	54.1
–C–O–C; –NH_2	Stretching	1655–1653	61.8	41.8	61.2	34.2	47.3	55.3
–NH_2	Bending	1561–1559	62.4	39.7	51.0	28.0	42.3	49.1
$O=\underset{I}{C}-O^-$; –NH_2	Stretching	1541	70.4	44.1	46.6	31.8	40.8	51.8
–C–O–C	Bending	1507	75.9	50.6	52.3	34.4	45.8	54.1
–CH_2	Bending	1459–1457	78.2	54.9	60.8	43.3	58.2	60.7
–CH_3–CH_2–	Bending in plane	1179–1161	62.2	33.1	59.6	33.1	42.8	49.8
–C–O–C–	Vibrating	1143	59.6	34.5	58.1	34.7	45.9	51.6
–CH_3–CH_2–; –C–O–C–	Stretching, vibrating	1057–1048	43.3	25.2	46.8	23.3	31.6	53.6
–CH_2; –C–H	Rocking; bend out plane	854–852	41.2	41.0	69.2	32.7	41.5	42.9
–CH_2; –C–H	Rocking; bend out plane	671–668	20.9	56.5	100.0	8.7	9.1	12.7

assumed as another evidence of successful encapsulation of *n*-hexadecane.

3.2. Leakage behavior

When the supernatant samples stayed overnight in the refrigerator at 4 °C following the centrifugal shear force test were checked, it was observed that almost all, except for Coacervates V and VI, included only the liquid phase of water and did not contain any exuded oil droplet, thus verifying no leakage. It is noteworthy that the durability of the coacervates, containing *n*-hexadecane and *n*-nonadecane, was essentially maintained. Supportively, no staining was detected on the fabric surfaces indeed during heating them in oven for fixation after coating. This might also be the indication for their durability as their incorporation into the fabrics. Therefore the developed encapsulation procedure of PCMs can be adequately recommended for textile applications and handling.

However, the supernatant sample of Coacervate VI was separated into two phases in the test tube and the frozen oil phase remained above the liquid phase of water clearly, whereas that of Coacervate V comprised only a few drops of oil. The oil phase separation was further occurred in the sample of Coacervate VI during its heating in the calorimeter test. This might happen since charged polymers in the colloid form were less likely to show sufficient bonding tendency to the relatively longer chain of hydrocarbons, parallel to the literature findings [7,36]. In consequence, the coacervation procedure should be modified for the encapsulation of *n*-octadecane especially for pH values, electrolyte concentrations and stirring rates.

3.3. Thermal properties of the coacervates and coacervate incorporated woven fabrics

3.3.1. DSC results of the coacervates

Heating results of DSC analyses, given in Figs. 5 and 6, show that all produced coacervates including Control perform considerable heat absorptions in between −20 °C and 10 °C, yielding peaks around −5 °C to +5 °C in relation to the existence of some water molecules adhered to the coacervates with weak hydrogen bonding. In addition, DSC curves of Coacervates I to III in Fig. 5 illustrate further substantial endothermic enthalpies in the interval of 11–25 °C, corresponding to the solid–liquid phase transition of *n*-hexadecane. Likewise, the suc-

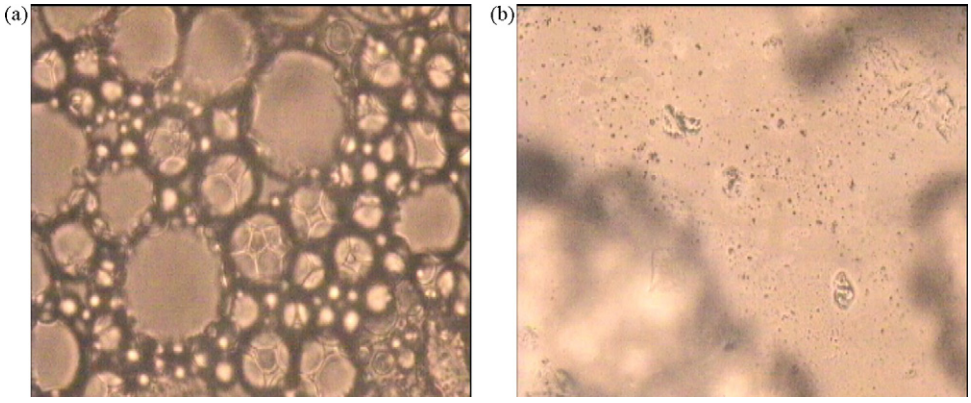

Fig. 4. Optical microscopic images of (a) Coacervate II and (b) control (magnification 100×).

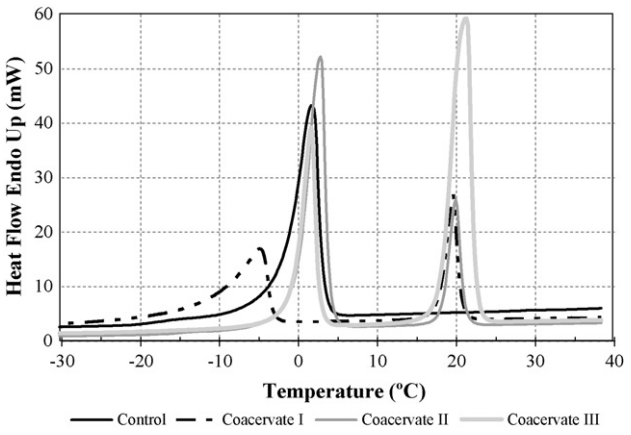

Fig. 5. The DSC curves of control, Coacervates I–III, all containing *n*-hexadecane, heated from −50 °C to 40 °C at 10 °C min^{-1} (sample weights are 5.6 mg, 6.2 mg, 5.2 mg and 7.0 mg, respectively).

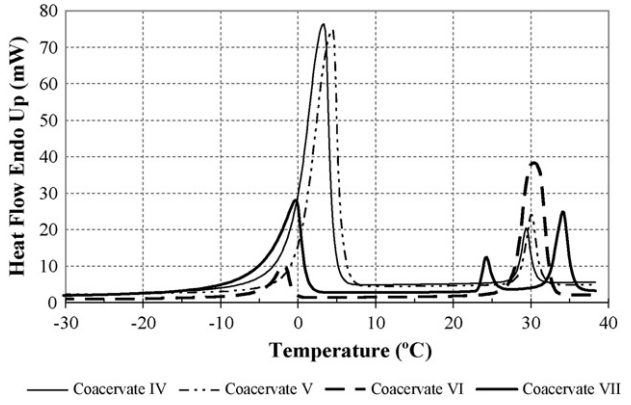

Fig. 6. The DSC curves of Coacervates IV–VI, all containing *n*-octadecane, and of Coacervate VII, containing *n*-nonadecane, heated from −50 °C to 40 °C at 10 °C min^{-1} (sample weights are 7.7 mg, 6.9 mg, 4.5 mg and 5.8 mg, respectively).

cesive endothermic changes in DSC curves of Coacervates IV to VI and VII in Fig. 6 greatly overlap with those of *n*-octadecane and *n*-nonadecane, respectively. The fact that Control does not present any supplementary heat absorption beyond melting point of water also reveals the achievement of PCM encapsulation by complex coacervation (see Fig. 5). Hence, results of DSC analyses verify the successful entrapping of PCMs in coacervates. Table 5 summarizes the phase transition characteristics of all coacervates containing paraffin waxes in between 5 °C and 40 °C.

Table 5
Phase transition characteristics of coacervates containing paraffin waxes in between 5 °C and 40 °C

Coacervate type	Transition intervals (°C)	Peak temperature (°C)	Enthalpy of transition, ΔH (J g^{-1})
Coacervate I	11–25	19.5	42.7
Coacervate II	13–22	19.9	50.3
Coacervate III	11–25	21.0	144.7
Coacervate IV	21–31	29.3	19.7
Coacervate V	25–32	30.0	30.2
Coacervate VI	21–35	30.3	165.8
Coacervate VII	22–27	24.3	13.3
	30–38	34.0	44.1

The main interest in fact is the enthalpy values of coacervates, practiced around the solid–solid and/or solid–liquid phase change temperatures of PCMs in DSC analyses, which are quite compatible for the textile applications. The absorbed energy levels of coacervates are proportional with those of PCMs for similar temperature intervals, and tend to increase whereas the dispersed PCM contents in emulsions are relatively higher. Considering the coacervates including low, medium and high percentages of *n*-hexadecane, Coacervate III performed the highest ΔH value of 144.7 J g^{-1} in between 11 and −25 °C, which was very close to that of *n*-hexadecane. Nevertheless, heat exertions of Coacervates I and II were also remarkable, 42.7 J g^{-1} and 50.3 J g^{-1}, respectively. This implies that relatively short chains of *n*-hexadecane ($C_{16}H_{34}$) were encapsulated quite successfully without any chemical decomposition. However, during complex coacervation of hydrophobic *n*-alkane, ionic charge balance of the mixture of Coacervate II could not probably be well-established and thus adversely affected the micelle formation, which resulted in a big differential between the enthalpies of Coacervates II and III.

Similarly, there is a good relationship between the enthalpies of Coacervates IV to VI and that of *n*-octadecane considering the amount of ingredient core materials in dispersions. Coacervate VI, corresponding to 80 percent *n*-octadecane addition, provided a significant enthalpy, say 165.8 J g^{-1}, in between 21 °C and −35 °C. ΔH values of Coacervates IV and V were relatively lower, 19.7 J g^{-1} and 30.2 J g^{-1}. To obtain better results at all core-shell material ratios, instantaneous changes in charge distribution can be minimized via adding surfactants at higher concentrations to the dispersion, which is critical for encapsulation of bigger molecules of *n*-octadecane ($C_{18}H_{38}$).

The DSC graph of Coacervate VII in Fig. 6 and that of *n*-nonadecane ($C_{19}H_{40}$) in Fig. 7 mutually represent similarities for their crystal-rotator and rotator-liquid transitions during heating. The distinct low temperature shoulder of $C_{19}H_{40}$ attributed to the rotator phase transition below the melting peak is apparent and common to all odd *n*-alkanes between C_9 and C_{45} [41]. On the other hand, the integral area of melting peak is approximately

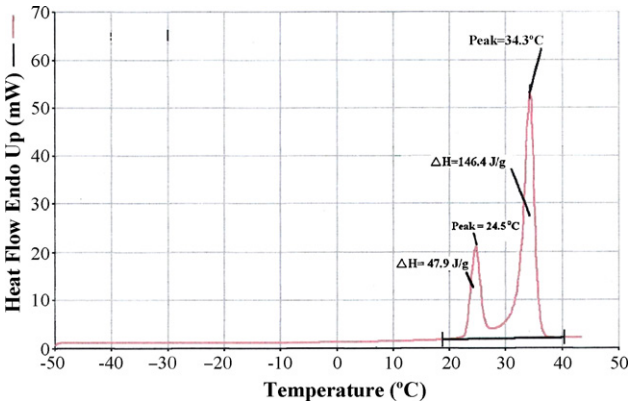

Fig. 7. The DSC curve of *n*-nonadecane (sample weight is 5.4 mg).

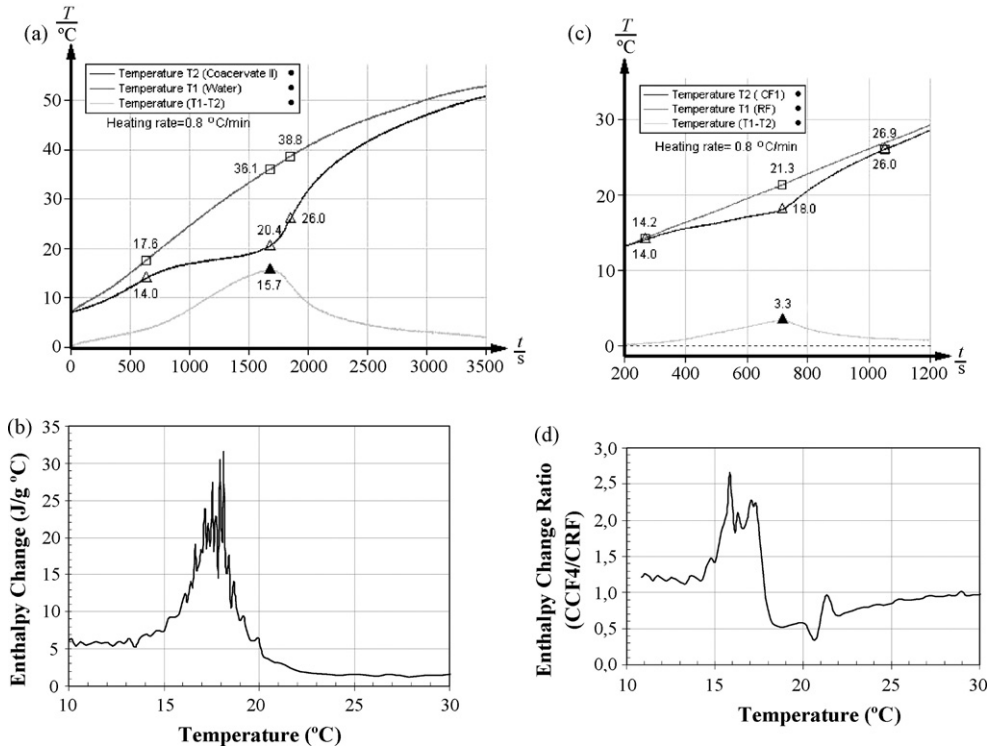

Fig. 8. (a) Calorimeter graph of the first replicate of Coacervate II; (b) enthalpy change curve of Coacervate II; (c) calorimeter graph of the fabric CF1,containing 9.5% of Coacervate II; (d) relative enthalpy change of the fabric CF1 to that of reference fabric (RF).

75% of the total heat absorption of $C_{19}H_{40}$. Matching peaks in DSC curve of Coacervate VII illustrate that typical phase transition characteristics have been conveyed after encapsulation of *n*-nonadecane. As given in Table 5, Coacervate VII yielded 13.3 J g^{-1} and 44.1 J g^{-1} in association with these crystal-rotator and rotator-liquid transitions.

Moreover, cooling experiments of coacervates showed important exothermic phase transitions at relatively lower tem-

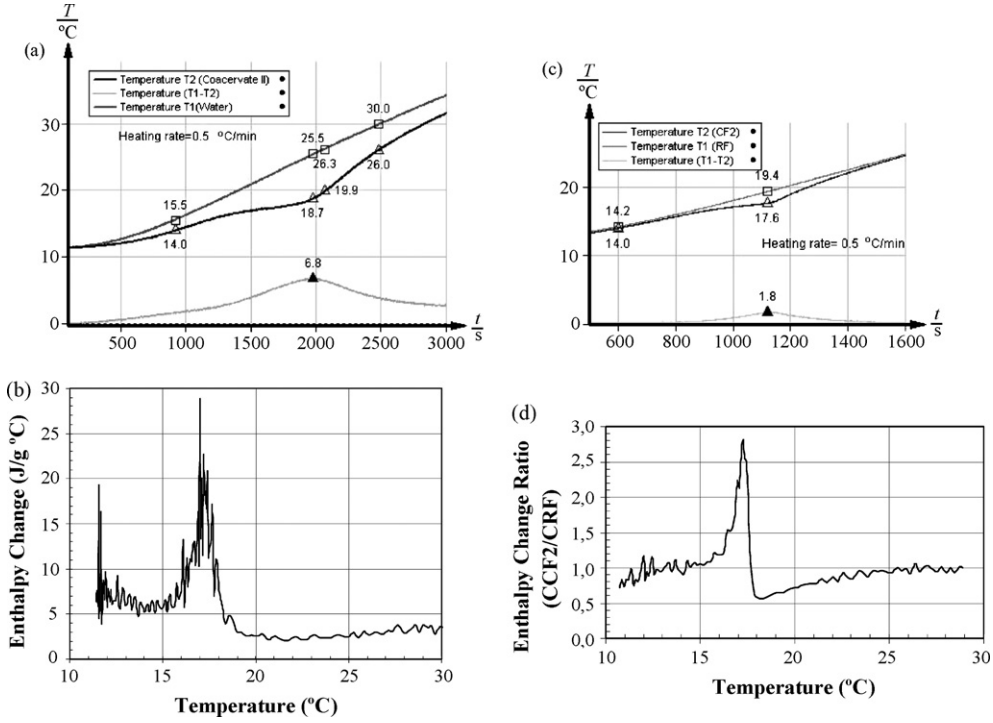

Fig. 9. (a) Calorimeter graph of the second replicate of Coacervate II; (b) enthalpy change of Coacervate II; (c) calorimeter graph of the fabric CF2, containing 15.6% of the second replicate of Coacervate II; (d). relative enthalpy change of the fabric CF2 to that of reference fabric (RF).

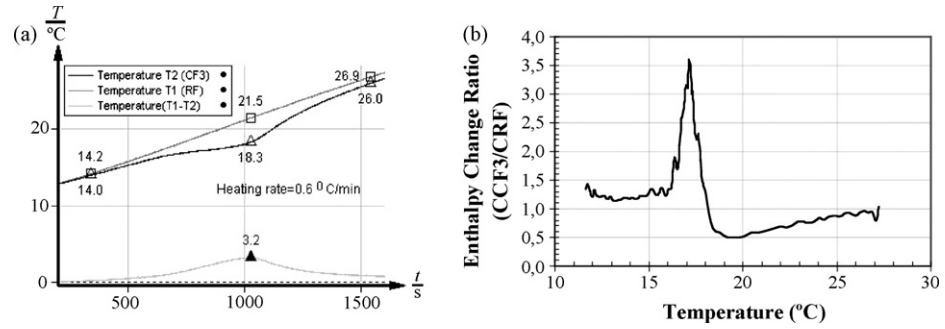

Fig. 10. (a) Calorimeter graph of the fabric CF3, containing 22.5% of the second replicate of Coacervate II and (b) relative enthalpy change of the fabric CF3 to that of reference fabric (RF).

perature ranges compared to heating. Since the transition of a disordered liquid phase to an ordered solid structure was rather difficult, super cooling happened, therefore peak temperatures shifted to 15.0 °C for Coacervates I to III (samples containing *n*-hexadecane), to 25.0 °C for Coacervates IV to VI (samples containing *n*-octadecane), and to 26.0 °C and 15.0 °C for Coacervate VII (the sample containing *n*-nonadecane).

3.3.2. Comparative results of the calorimeter measurements of the coacervates and coacervate incorporated fabrics

Figs. 8–11 show thermal measurement results of the coacervates alone and incorporated into the fabrics comparatively in calorimeter tests.

Figs. 8a, 9a and 11a show temperature (T/°C) versus time (t/s) plots of coacervates reference to distilled water. The general tendency arising from these low rate heating curves is the decelerated temperature changes for the coacervate in an interval greatly overlapping the phase transition interval of *n*-hexadecane, while that of water runs upward with more or less constant pace even though the consumed energy per second for each is almost the same. Assigned points of phase transition and the maxima on coacervate curves are in accordance with the related DSC results. Following the phase change, temperature increases accelerate and close up to that of water.

Enthalpy change of each coacervate in terms of J g^{-1} °C^{-1} is the one derived from immediate heat absorption of the same amount of water of 4.18 J g^{-1} °C^{-1} specific heat capacity (See Figs. 8b, 9b and 11b). In between 14.0 and −26.0 °C, Coacervate III and two replicates of Coacervate II performed enthalpies as 178 J g^{-1}, 164 J g^{-1}, and 101 J g^{-1}, respectively. Coacervate III yielded the best result which also emphasized by the maximum temperature difference attained ($T_1 - T_2 = 17.4$ °C) in Fig. 11a. However, the repeated experiments conducted for Coacervate II show that their thermal improvements are also sound and can be modified by improving the accuracy of trial.

Figs. 8c, 9c, 10a and 11c demonstrate temperature versus time graphs for the coated fabric samples, CF1 to CF4, reference to uncoated fabric sample, RF. Similar reclining biases within alike intervals for the curves of CF1 to CF4 are observed concerning those of their coacervates in Figs. 8a, 9a and 11a; whilst RF

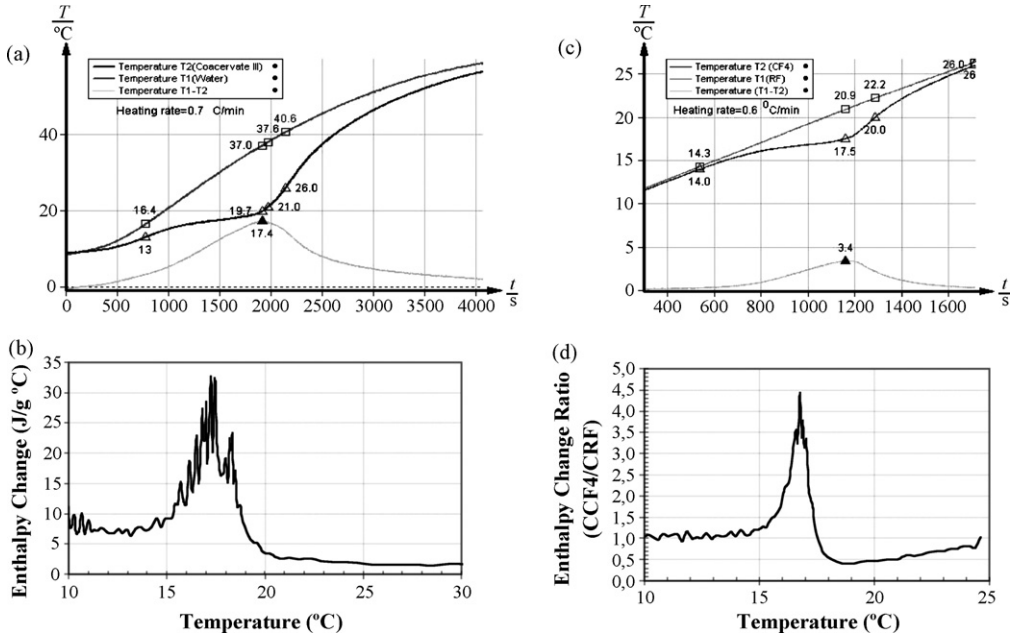

Fig. 11. (a) Calorimeter graph of Coacervate III; (b) enthalpy change curve of Coacervate III; (c) calorimeter graph of the fabric CF4, containing 9.5% of Coacervate III; (d) relative enthalpy change of the fabric CF4 to that of reference fabric (RF).

curves follow a line inclined upward. The performances accomplished for the coated fabric samples are related to both actual *n*-hexadecane content of the particular coacervate and the incorporation amount of it by the coating application, changing from 9.5% to 22.5% in the study, which eventually determine the resultant PCM content of the fabric. Figs. 9c and 10a emphasize the distinction in the enthalpy values of the coated fabric samples CF2 and CF3 because the incorporated coacervate percentage is raised from 15.6 to 22.5, although they are prepared from the second replicate of Coacervate II.

Figs. 8d, 9d, 10b and 11d express the enthalpy change ratios of coated and uncoated fabrics, c_{CF1}/c_{RF} to c_{CF5}/c_{RF} ($J\,g^{-1}\,^{\circ}C^{-1}/J\,g^{-1}\,^{\circ}C^{-1}$), derived from ΔT values of the samples of equal mass which absorbed almost the same energy per second. Ratios arrive to remarkable peak values varying within a range from 2.5 to 4.5 which means that the energy absorption capacity of the coacervate added fabric can be 2.5–4.5 times enhanced relative to the reference fabric for particular temperature intervals. Figs. 8d and 11d underline the further enhancement in the enthalpy values of CF4 with respect to that of CF1, depending on the increase in the dispersed content of *n*-hexadecane in the emulsion from 60% to 80% for the trials of Coacervates II and III.

4. Conclusion

The complex coacervation method used in this study has been succeeded to encapsulate paraffin waxes of high heat storage capacities by means of natural and biodegradable polymers, namely gelatin and gum arabic. The coacervates, manufactured for *n*-hexadecane and *n*-octadecane, each included by low, medium and high percentages and *n*-nonadecane included by medium percentage, have performed their functions of energy absorption perfectly during their heating at different rates, say 0.5–1 and 10 $^{\circ}C\,min^{-1}$ in calorimeter and DSC tests. The achieved enthalpies were found proportional to those of hydrocarbons in temperature intervals corresponding to the phase transitions of PCMs. Thus, the enthalpy value of the coacervate within a certain interval, as a measure of thermal enhancement, could be raised significantly by increasing the dispersed content of PCM in the emulsion up to 80%, i.e. 144 $J\,g^{-1}$ for Coacervate III containing *n*-hexadecane and 165.8 $J\,g^{-1}$ for Coacervate VI containing *n*-octadecane in DSC analyses, characterizing the big proportionate of the thermal performance of pure PCMs. Consequently, heat storage performances of coacervates were very satisfactory for both 60% and 80% dispersion ratios of PCMs.

FT-IR results have presented the proofs of successful complex coacervation of PCMs. Moreover, three types of coacervates, Coacervates I–III comprising *n*-hexadecane, withstood considerable centrifugal forces in the leakage test and compression in coating applications of fabrics without resulting in any oil leak. Although the findings for the durability of Coacervate IV and VII, comprising low and medium content *n*-octadecane and *n*-nonadecane, respectively, were completely in the same direction. The results obtained from centrifugal force test and from heating test in calorimeter for Coacervate VI with the high concentration of *n*-octadecane lead to us a conclusion that the leakage behavior of the encapsulated PCMs becomes more critical for relatively longer chains of hydrocarbons and the coacervation needs to be modified to avoid the lack of oil by taking into account the process parameters, i.e. more precise pH value, amount and concentration of surfactants and higher stirring rates.

The thermal enhancement of the fabrics could be achieved by incorporating some of the coacervates through coating, the technique which is commonly used to modify textile surfaces. The attained performances varied depending on actual PCM content of the coacervate and its ratio in the coating mixture as well as the applied amount of coating material on the fabric. However, in all cases, the temperature of the coated sample remained significantly lower than the reference fabric in phase change intervals under the constant heating conditions in calorimeter tests. On the contrary, the temperature of a PCM included fabric would relatively stay upper than that of reference in a cooling environment. For the studied coacervate percentages of fabrics, changing from 9.5% to 22.5%, the energy absorption capacities could be improved by 2.5–4.5 times relative to the references for particular temperature intervals. This implies the considerable contribution of the encapsulated PCM to the active thermal insulation of the fabric. Nevertheless, the thermal management practices of fabrics are not limited to the achievements in laboratory conditions. Improved performances for thermal capacity as well as serviceability can be executed in consequence of the high accuracy of trials and the advanced coating facilities in industrial applications. In conclusion, the complex coacervation of gelatin–GA to encapsulate paraffin waxes and their incorporation into woven fabrics by coating can be fairly recommended to enrich the thermal performance of textile products, taking into account their high thermal storage densities, durability and easy application to a fabric surface.

Acknowledgements

We would like to thank METU Central Laboratory for their contribution to FT-IR and DSC analysis, CHT-Turkey for providing coating material used in the experimental study.

References

[1] D.P. Colvin, Y.G. Bryant, J.C. Driscoll, J.C. Mulligan, Thermal insulating coating employing microencapsulated phase change material and method, US Patent 58,04,297 (1998) available from http://patft.uspto.gov/.
[2] F.R. Chamberlain, J.A. Agostinelli, H.J. Gysling, Thermally protective camera case, US Patent 63,77,755 (2002) available from http://www.freepatentsonline.com/.
[3] G.A. Lane, Low temperature heat storage with phase change materials, Int. J. Ambient Energy 1 (1980) 155–168.
[4] I.O. Salyer, O. Ival, Dry powder mixes comprising phase change materials, US Patent 51,06,520 (1992) available from http://www.freepatentsonline.com/.
[5] Y. Hong, G. Xin-shi, Preparation of polyethylene–paraffin compounds as a form-stable solid–liquid phase change material, Solar Energy Mater. Solar Cells 64 (2000) 37–44.
[6] M.N.A. Hawlader, M.S. Uddin, M.M. Khin, Microencapsulated PCM thermal-energy storage system, Appl. Energy 74 (2003) 195–202.
[7] N. Sarier, E. Onder, The manufacture of microencapsulated phase change materials suitable for the design of thermally enhanced fabrics, Thermochim. Acta 452 (2) (2007) 149–160.

[8] P. Schossig, H.M. Henning, S. Gschwander, T. Haussmann, Microencapsulated phase-change materials integrated into construction materials, Solar Energy Mater. Solar Cells 89 (2005) 297–306.
[9] P. Stark, PCM-impregnated polymer microcomposites for thermal energy storage, SAE (Soc. Automotive Eng.) Trans. 99 (1990) 571–588.
[10] R.M. Carn, Phase change material blend, method for making, and devices using same, US Patent 66,52,771 (2003) available from http://www.freepatentsonline.com/.
[11] T.A. Lowrey, A. Tyler, Phase change material memory device, US Patent 65,86,761 (2003) available from http://www.freepatentsonline.com.
[12] M.M. Farid, A.M. Khudhair, S.A.K. Razack, S. Al-Hallaj, A review on phase change energy storage: materials and applications, Energy Convers. Manage. 45 (2004) 1597–1615.
[13] B. Zalba, J. Marin, L.F. Cabeza, H. Mehling, Review on thermal energy storage with phase change: materials, heat transfer analysis and applications, Appl. Therm. Eng. 23 (2003) 251–283.
[14] C. Alkan, Enthalpy of melting and solidification of sulfonated paraffins as phase change materials for thermal energy storage, Thermochim. Acta 451 (1/2) (2006) 126–130.
[15] Z. Liu, D.D.L. Chung, Calorimetric evaluation of phase change materials for use as thermal interface materials, Thermochim. Acta 366 (2) (2001) 135–147.
[16] K. Junghye, C. Gilsoo, Thermal storage/release, durability, and temperature sensing properties of thermostatic fabrics treated with octadecane-containing microcapsules, Text. Res. J. 72 (12) (2002) 1093–1098.
[17] M.H. Hartmann, M.C. Magill, Melt spinable concentrate pellets having enhanced reversible thermal properties, US Patent 67,93,856 (2004) available from http://www.freepatentsonline.com/.
[18] E.N. Brown, M.R. Kessler, N.R. Sottos, S.R. White, In situ poly (urea–formaldehyde) microencapsulation of dicyclopentadiene, J. Microencapsul. 20 (6) (2003) 719–730.
[19] G. Nelson, Application of microencapsulation in textiles, Int. J. Pharm. 242 (2002) 55–62.
[20] K. Choi, G. Cho, P. Kim, C. Cho, Thermal storage/release and mechanical properties of phase change materials on polyester fabrics, Text. Res. J. 74 (4) (2004) 292–297.
[21] J.C.H. Chen, J.L. Eichelberger, Method for preparing encapsulated phase change materials, US Patent 45,05,953 (1985) available from http://patft.uspto.gov/.
[22] P.L. Foris, R.W. Brown, J. Phillips, S. Paul, Capsule manufacture, US Patent 41,00,103 (1978) available from http://patft.uspto.gov/.
[23] L.A. Luzzi, Microencapsulation, J. Pharm. Sci. 59 (10) (1970) 1367–1376.
[24] H. Kawai, Hideyuki, K. Anan, M. Matsumoto, M. Kushino, Microcapsule and its uses, US Patent 71,47,915 (2006) available from http://www.freepatentsonline.com.
[25] B.K. Green, Oil containing microscopic capsules and method making them, US Patent 28,00,458 (1957) available from http://www.freepatentsonline.com.
[26] G.F. Sachel, Method of encapsulating liquids, US Patent 32,02,533 (1965) available from http://www.freepatentsonline.com.
[27] IUPAC, Compend. Chem. Terminol. 31 (1972) 611.
[28] J.R.P. Bishop, G. Nelson, J. Lamb, Microencapsulation in yeast cells, J. Microencapsul. 15 (6) (1998) 761–773.
[29] V. Ducel, J. Richard, P. Saulnier, Y. Popineau, F. Boury, Evidence and characterization of complex coacervates containing plant proteins: applications to the microencapsulation of oil droplets, Colloid Surf. A 232 (2004) 239–247.
[30] C.G. de Kruif, F. Weinbreck, R. de Vries, Complex coacervation of proteins and anionic polysaccharides, Curr. Opin. Colloid Interface 9 (5) (2004) 340–349.
[31] Y. Özonur, M. Mazman, H.Ö. Paksoy, H. Evliya, Microencapsulation of coco fatty acid mixture for thermal energy storage with phase change material, Int. J. Energy Res. 30 (10) (2006) 741–749.
[32] X.X. Zhanga, Y.F. Fana, X.M. Taob, K.L. Yickb, Fabrication and properties of microcapsules and nanocapsules containing *n*-octadecane, Mater. Chem. Phys. 88 (2004) 300–307.
[33] H.G. Bungenberg de Jong, H.R. Kruyt, Coacervation (partial miscibility in 17 colloid systems), Proc. Kon. Ned. Akad. Wet. 32 (1929) 849–856.
[34] Y. Vinetsky, S. Magdassi, Microencapsulation by surfactant–gelatin insoluble complex: effect of pH and surfactant concentration, J. Colloid Interface Sci. 189 (1) (1997) 83–91.
[35] K. Nakagawa, S. Iwamoto, M. Nakajima, A. Shono, K. Satoh, Microchannel emulsification using gelatin and surfactant-free coacervate microencapsulation, J. Colloid Interf. Sci. 278 (1) (2004) 198–205.
[36] N. Sarier, E. Onder, Thermal characteristics of polyurethane foams incorporated with phase change materials, Thermochim. Acta 454 (2) (2007) 90–98.
[37] IUPAC, Compend. Chem. Terminol. 66 (1994) 589.
[38] K. Hong, S. Park, Melamine resin microcapsules containing fragrant oil: synthesis and characterization, Mater. Chem. Phys. 58 (1999) 128–131.
[39] B. Henkel, E. Bayer, Monitoring of solid phase peptide synthesis by FT-IR spectroscopy, J. Pept. Sci. 4 (8) (1998) 461–470.
[40] S.C.Szu, R. Schneerson, J.B. Robbins, Polysaccharide–protein conjugates, US Patent 52,04,098 (1993) available from http://www.freepatentsonline.com/.
[41] X. Zhang, Y. Fan, X. Tao, K. Yick, Crystallization and prevention of supercooling of microencapsulated *n*-alkanes, J. Colloid Interface Sci. 281 (2005) 299–306.